THREE-DIMENSIONAL ANALYSIS OF MAGNETODYNAMIC FIELDS IN ELECTROMAGNETIC DEVICES TAKEN INTO ACCOUNT THE DYNAMIC HYSTERESIS LOOPS

Yoshifuru Saito

Abstract - A new magnetic field equation exhibiting dynamic hysteresis loops is proposed. Based on this magnetic field equation, a system of two-dimensional magnetic circuit equations taken into account the dynamic hysteresis loops is derived by the method of magnetic circuits. By means of magnetic power invariant transformation, a system of two-dimensional magnetic circuit equations is transformed into a system of three-dimensional magnetic circuit equations. This system of three-dimensional magnetic circuit equations is discretized in time by a finite difference method. A system of three-dimensional magnetic circuit equations discretized in time is solved by a simple iteration method, using a relaxation parameter.

As an example, a system of three-dimensional magnetic circuit equations of a simple saturable reactor is derived. Also, the numerical solutions of dynamic hysteresis loops in a saturable reactor are presented together with those of experimental results.

INTRODUCTION

With the development of modern computers, numerical methods became available to calculate the magnetic fields in electromagnetic devices. Since the iron parts in electromagnetic devices constitute the major magnetic flux paths, the magnetization characteristic of iron becomes of paramount importance in calculating the magnetic fields in electromagnetic devices. The magnetization characteristic of iron is essentially nonlinear, and is classified into two-properties: one is the magnetic saturation, and the other is the magnetic hysteresis. Particularly, in these magnetization properties, the magnetic hysteresis plays an important role in the magnetic field distributions in electromagnetic devices.

The principal purpose of this paper is to derive the simplest empirical magnetic field equation exhibiting the dynamic hysteresis loops, and to develop the theory of magnetic circuits as a means of solving the three-dimensional magnetic field problems in electromagnetic devices. As a concrete example, a system of three-dimensional magnetic circuit equations of a simple saturable reactor is derived, taking into account the eddy currents as well as dynamic hysteresis loops. Also, the numerical solutions of dynamic hysteresis loops in a satuarable reactor are presented together with those of experimental results.

MAGNETIC FIELD EQUATION EXHIBITING THE DYNAMIC HYSTERESIS LOOPS

Figure 1(a) shows a typical magnetic hysteresis loop. When we consider an arbitrary point (H_a,B_a) in Fig. 1(a), then it is possible to consider that the magnetic field intensity H_a is composed of two magnetic field intensities H_μ and H_s, that is

$$H_a = H_\mu + H_s . \tag{1}$$

The relationship between the magnetic field intensity H_μ and magnetic flux density B_a is assumed to take the following form:

$$H_\mu = (1/\mu)B_a , \tag{2}$$

The author is with College of Engineering, Hosei University, 3-7-2 Kajinocho Koganei, Tokyo 184, Japan.

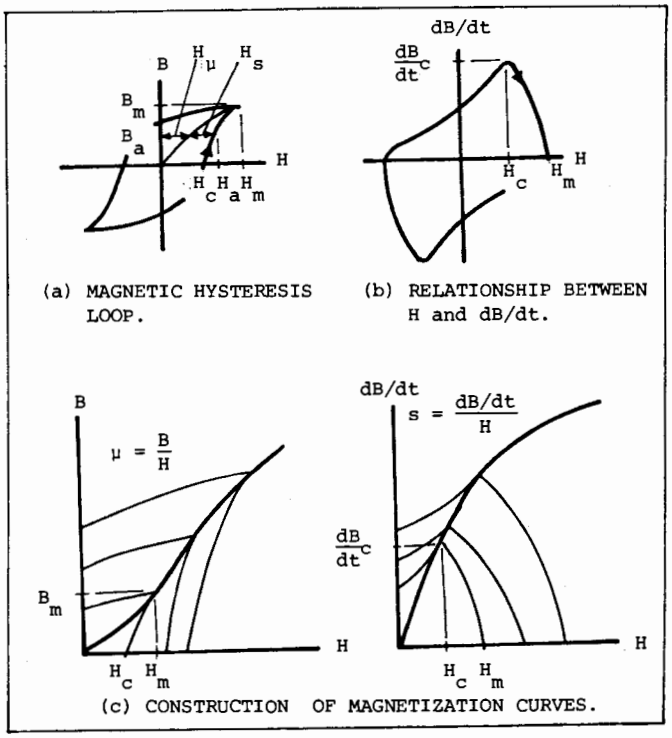

Fig. 1. Dynamic hysteresis model.

where μ denotes the magnetic permeability of iron.

When the permeability μ is introduced into (2) as a function of the magnetic field intensity H_μ or magnetic flux density B_a, then (2) represents the magnetic saturation property of iron. Therefore, the remaining term H_s has to represent the dynamic hysteresis property. Therefore, at least, the magnetic field intensity H_s has to satisfy the following conditions: (1) when the magnetic flux density B is increasing from $-B_m$ to $+B_m$, then H_s must take the positive values, (2) when the magnetic flux density B is decreasing from $+B_m$ to $-B_m$, then H_s must take the negative values, (3) when the magnetic flux density B reaches to the positive or negative maximum value $\pm B_m$, then H_s must die out, and (4) the area bounded by the hysteresis loop must be equivalent to the hysteresis loss energy per unit volume. Figure 1(b) shows the relationship between the magnetic field intensity H and time derivative of magnetic flux density B. By considering the above conditions (1)-(4) and Figs. 1(a),1(b), it is possible to assume that the magnetic field intensity H_s depends on the rate of change of magnetic flux density B_a in time t, that is

$$H_s = (1/s)(dB_a/dt), \tag{3}$$

where the hysteresis coefficient s is introduced to relate H_s with dB_a/dt, and has the unit of ohm per meter. The magnetic hysteresis loss power P_a (watt per volume) at a point (H_a,B_a) in Fig. 1(a) is given by

$$P_a = H_s(\frac{dB}{dt}a) = (\frac{1}{s})(\frac{dB}{dt}a)^2 . \tag{4}$$

By means of (1)-(3), the magnetic field equation exhibiting the dynamic hysteresis loops is assumed to take the following form:

0018-9464/82/0300-0546$00.75 © 1982 IEEE

$$H = (\frac{1}{\mu})B + (\frac{1}{s})\frac{dB}{dt} . \quad (5)$$

(5) exhibits many typical hysteresis characters such as the presence of minor loops and increase in area bounded by the loop with frequency, because (5) is essentially similar in form to those of Charap and Chua [1-3].

When we consider the peak point (H_m,B_m) in Fig. 1(a), then the permeability μ_m can be calculated by $\mu_m=B_m/H_m$, because the time derivative of magnetic flux density B in Fig. 1(b) is reduced to zero at the point (H_m,B_m) in Fig. 1(a). Also, the hysteresis coefficient s_c can be calculated by $s_c=(dB_c/dt)/H_c$, because the magnetic flux density B in Fig. 1(a) is reduced to zero at the point $(H_c,dB_c/dt)$ in Fig. 1(b). Similarly, the permeabilities and hysteresis coefficients in the other points can be obtained, and their results construct the magnetization curves as shown in Fig. 1(c).

THEORY OF MAGNETIC CIRCUITS IN TWO-DIMENSIONAL FIELDS

Consider the region bounded by the contour $\overline{abcda}$ in Fig. 2(a), it is possible to write the fundamental relation between the magnetic field intensity H and current density J_1 as

$$\int_{\overline{abcda}} H dl = \int_{S_{\overline{abcda}}} J_1 . nda , \quad (6)$$

where dl denotes the infinitesimally small distance along the contour $\overline{abcda}$, da is the infinitesimally small area, $S_{\overline{abcda}}$ is the surface area bounded by the contour $\overline{abcda}$, and n is the unit normal vector on the infinitesimally small area da. Moreover, subscripts 1,2,3,4,5 refer to the mesh points in Fig. 2(a). The right-hand term in (6) is equivalent to the current i_1 flowing through the surface $S_{\overline{abcda}}$, viz.

$$\int_{S_{\overline{abcda}}} J_1 . nda = i_1 . \quad (7)$$

By considering (5),(6), the left-hand term in (6) is rewritten by

$$\int_{\overline{abcda}} H dl = \int_{\overline{abcda}} [(\frac{1}{\mu})B + (\frac{1}{s})\frac{dB}{dt}] dl . \quad (8)$$

In order to apply the method of magnetic circuits to the magnetic field regions in Fig. 2(a), it is assumed that the current i_1 in (7) is not uniformly distributed on the surface $S_{\overline{abcda}}$, but concentrated on the conductor with infinitesimally small cross-sectional area located at the mesh point of the surface $S_{\overline{abcda}}$. Similarly, it is assumed that the currents in the other regions in Fig. 2(a) are concentrated on the conductors with infinitesimally small cross-sectional area located at each of their mesh points. Due to the nonlinear magnetization characteristic of iron, it is assumed that the permeability μ as well as hysteresis coefficient s in (8) may take different values with respect to the positions. Moreover, it is assumed that the magnetic field intensity H and magnetic flux density B along the contour $\overline{abcda}$ in Fig. 2(a) may take different values, but the magnetic flux which takes the paths along the contours $\overline{ab},\overline{bc},\overline{cd},\overline{da}$ may take a constant value. With these assumptions, the magnetic fields in Fig. 2(a) may be calculated for a modified form in the regions as shown in Fig. 2(b). In Fig. 2(b), let $\phi_1,\phi_2,\phi_3,\phi_4,\phi_5$ denote the loop magnetic fluxes, and let e_1 denote the externally impressed voltage in the direction of z-axis in Fig. 2(a), then the current i_1 in (7) and the right-hand term in (8) are rewitten by

$$i_1 = (1/r_1)[e_1 - (d/dt)\phi_1] , \quad (9)$$

$$\int_{\overline{abcda}} [(\frac{1}{\mu})B + (\frac{1}{s})\frac{dB}{dt}] dl = \sum_{k=2}^{5} [R_{1k} + S_{1k}(\frac{d}{dt})][\phi_1 - \phi_k] , \quad (10)$$

where r_1 is the electric resistance defined in the direction of z-axis; R_{1k} and S_{1k} are respectively the magnetic resistance and hysteresis parameter defined along the contour $\overline{abcda}$ as shown in Fig. 2(c). The magnetic resistance calculations with various geometrical shapes are described in [4]. By considering (10), it is found that the parameter which depends on the geometrical shape is common to R_{1k} and S_{1k}. Therefore, the hysteresis parameters with various geometrical shapes are calculated in much the same way as the magnetic resistance. Also, the electric resistance r_1 in (9) is calculated in much the same way as the magnetic resistance, because the definition of electric resistance with respect to the geometrical shape is similar to the definition of magnetic resistance [4,5].

By means of (9),(10), the two-dimensional magnetic circuit equation is formally written by

$$(\frac{1}{r_1})[e_1 - (\frac{d}{dt})\phi_1] = \sum_{k=2}^{5} [R_{1k} + S_{1k}(\frac{d}{dt})][\phi_1 - \phi_k] . \quad (11)$$

The Appendix shows that (11) is one of the finite difference equations.

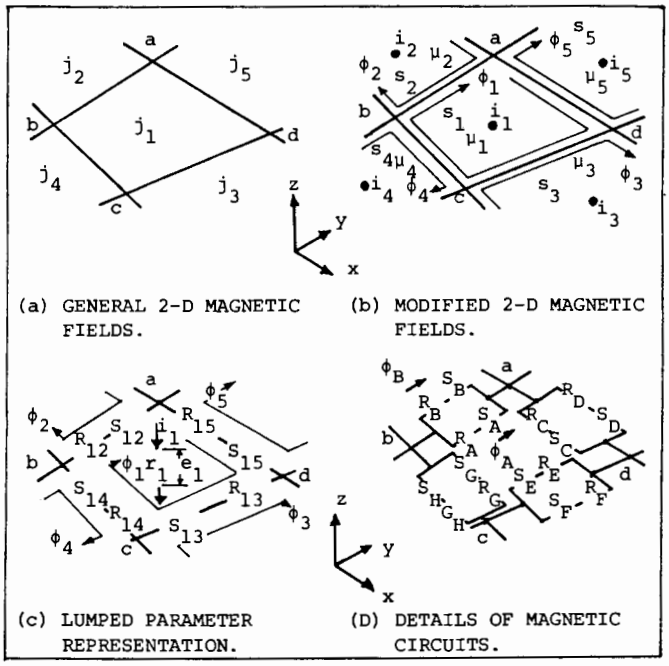

Fig. 2. Two-dimensional fields.

For computational convenience, it is preferable to assume that the region which encloses each of the mesh points in Fig. 2(b) may have the distinct permeability and hysteresis coefficient. Thereby, it is assumed that the magnetic fields in Fig. 2(a) may be calculated from the magnetic circuits shown in Fig.2(d) . Let $F_{\overline{ab}}$ denote the magnetomotive force between the node a and b in Fig. 2(d), then it is possible to write the following relation:

$$\phi_1 - \phi_2 = \phi_A + \phi_B = \frac{1}{R_A}[F_{\overline{ab}} - S_A(\frac{d\phi}{dt}A)] + \frac{1}{R_B}[F_{\overline{ab}} - S_B(\frac{d\phi}{dt}B)] , \quad (12)$$

where ϕ_1,ϕ_2 are shown in Fig. 2(c); $\phi_A,\phi_B,R_A,R_B,S_A,S_B$ are shown in Fig. 2(d). When the time derivatives of diverted magnetic fluxes ϕ_A,ϕ_B are given by

$$\frac{d\phi_A}{dt} = \frac{R_B}{R_A+R_B}\left(\frac{d}{dt}\right)[\phi_1 - \phi_2] , \quad (13)$$

$$\frac{d\phi_B}{dt} = \frac{R_A}{R_A+R_B}\left(\frac{d}{dt}\right)[\phi_1 - \phi_2] , \quad (14)$$

then the magnetic impedance between the node a and b in Fig. 2(c) can be represented in terms of the circuit parameters in Fig. 2(d) as

$$R_{12}+S_{12}\left(\frac{d}{dt}\right) = \frac{R_A R_B}{R_A+R_B} + \left[\left(\frac{R_B}{R_A+R_B}\right)^2 S_A + \left(\frac{R_A}{R_A+R_B}\right)^2 S_B\right]\left(\frac{d}{dt}\right) . \quad (15)$$

The other circuit parameters in Fig. 2(c) can be similarly represented in terms of the circuit parameters in Fig. 2(d).

When we consider that the diverted magnetic flux depends only the magnetic resistance R_A, R_B in Fig. 2(d), then the magnetic field energy w_A stored in the magnetic resistance R_A is given as $w_A=(1/2)R_A[R_B(\phi_1-\phi_2)/(R_A+R_B)]^2$. Similarly, the magnetic field energies w_C, w_G, w_E stored in the magnetic resistances R_C, R_G, R_E in Fig. 2(d) can be obtained in much the same way as W_A. By adding these magnetic field energies, the total magnetic field energy $w_{\overline{abcda}}$ stored in the region taking the permeability μ_1 in Fig. 2(b) is given by

$$w_{\overline{abcda}} = w_A + w_C + w_E + w_G = \left(\frac{1}{2\mu_1}\right)B^2 V_{\overline{abcda}} , \quad (16)$$

where $V_{\overline{abcda}}$ denotes the volume of the region taking the permeability μ_1 and hysteresis coefficient s_1 in Fig. 2(b). By means of (16), it is possible to determine the permeability μ_1 as a function of the magnetic field intensity $(B/\mu_1)=\sqrt{2w_{\overline{abcda}}/(\mu_1 V_{\overline{abcda}})}$.

By means of (4), (13), the hysteresis power dissipated in the hysteresis parameter S_A is given as $p_A=(1/2)S_A\{[R_B/(R_A+R_B)](d/dt)(\phi_1-\phi_2)\}^2$. Similarly, the hysteresis powers p_C, p_E, p_G dissipated in the hysteresis parameters S_C, S_E, S_G in Fig. 2(d) can be obtained in much the same way as p_A. Thereby, the hysteresis coefficient s_1 can be obtained as a function of the magnetic field intensity $(1/s_1)(dB/dt) = \sqrt{2p_{\overline{abcda}}}/(s_1 V_{\overline{abcda}})$, where $p_{\overline{abcda}}=p_A+p_C+p_E+p_G$.

THEORY OF MAGNETIC CIRCUITS IN THREE-DIMENSIONAL FIELDS

Most electromagnetic devices consist of conducting wires around an iron core, in order to minimize the magnetic field energy stored in the iron core, the eddy currents in the iron core flow in a direction opposite to the exciting current. The magnetic flux which passes through the path parallel to the current-carrying coil can be neglected, therefore, it is preferable to consider the solid element as shown in Fig. 3(a). The permeability and hysteresis coefficient of this solid elememt are determined from the magnetic field intensities in the radial and in the tangential directions. Also, the central portion of the solid element in Fig. 3(a) is one of the solid elements; the permeability and hysteresis coefficient of this element become the functions of magnetic field intensities in the tangential direction, because the magnetic resistance in the radial direction reaches an infinitely large value.

For simplicity, it is preferable to consider a concrete example. One of the simplest examples of electromagnetic devices is the saturable reactor as shown in Fig. 3(b). This saturable reactor is divided into M_R parts in the radial direction and M_T parts in the tangential direction, taking into account the region containing air. Thereby, the magnetic field calculation of the saturable reactor is reduced to

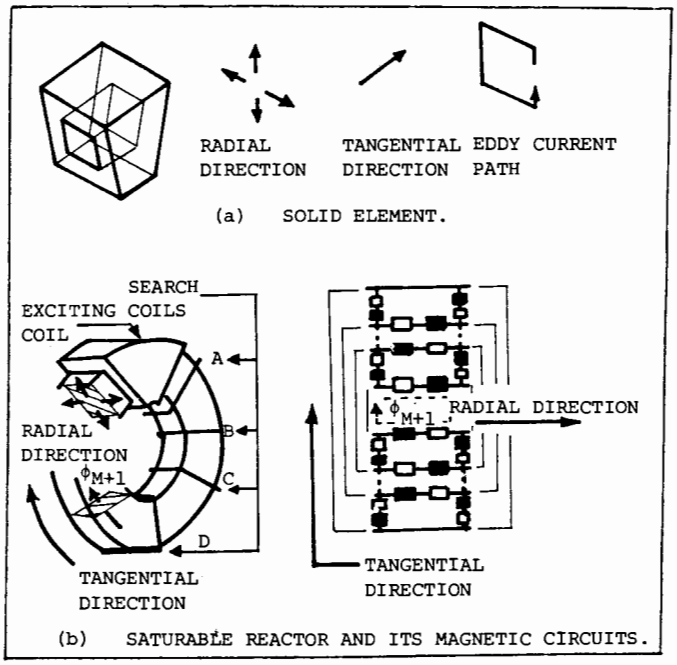

Fig. 3. Solid element and saturable reactor.

evaluate the $M(=M_R \times M_T)$ loop magnetic fluxes. Moreover, it is assumed that each of the exciting and search coils takes a distinct solid element which is similar in shape to the solid element shown in Fig. 3(a), and that no magnetic flux flows out of the boundary regions. The system of magnetic circuit equations is preferably expressed in matrix notation involving the externally impressed magnetomotive force vector $F[t]$, magnetic impedance matrix $Z[t]$ and magnetic flux vector $\Phi[t]$. After introducing the relationship between the number of turns of coil and magnetic flux linkage into (11), and rearranging, the system of magnetic circuit equations is expressed by

$$F[t] = Z[t]\Phi[t] , \quad (17)$$

where each of the matrices including the notation [t] is composed of the time varying elements. For notational convenience, let the subscript 1 refer to the quantities related to the exciting coil. The magnetic flux vector $\Phi[t]$ which is a column matrix of order M is written by

$$\Phi[t] = [\phi_1, \phi_2, \ldots, \phi_M]^T , \quad (18)$$

where the superscript T denotes the transpose of the matrix. The externally impressed magnetomotive force vector $F[t]$ involves the externally impressed voltage vector $V[t]$, electric conductance matrix G and winding matrix W, that is

$$F[t] = WGV[t] . \quad (19)$$

The externally impressed voltage vector $V[t]$ is a column matrix of order M, viz.

$$V[t] = [e_1, 0, \ldots, 0]^T , \quad (20)$$

where e_1 denotes the externally impressed voltage. The electric conductance matrix G and winding matrix W are the diagonal matrices of order M, that is

$$G = \text{diag.}\left[\frac{1}{r_1}, \frac{1}{r_2}, \ldots, \frac{1}{r_M}\right] , \quad (21)$$

$$W = \text{diag.}\,[N_1, 1, \ldots, 1] , \quad (22)$$

where r_1, r_2, r_M are respectively the electric resistances related to the loop magnetic fluxes ϕ_1, ϕ_2, ϕ_M; N_1 denotes the number of turns of the exciting coil.

The magnetic impedance matrix Z[t] consists of the magnetic resistance matrix R[t], hysteresis parameter matrix S[t], electric conductance matrix G and winding matrix W, viz.

$$Z[t] = R[t] + (S[t] + WGW)(d/dt) \ , \tag{23}$$

where

$$R[t] = \begin{vmatrix} R_{11} & -R_{12} & \cdot & \cdot \\ & R_{22} & \cdot & \cdot \\ & & \cdot & \cdot \\ \text{SYMMETRIC} & & & R_{MM} \end{vmatrix} , \tag{24}$$

$$S[t] = \begin{vmatrix} S_{11} & -S_{12} & \cdot & \cdot \\ & S_{22} & \cdot & \cdot \\ & & \cdot & \cdot \\ \text{SYMMETRIC} & & & S_{MM} \end{vmatrix} , \tag{25}$$

where the elements R_{11}, R_{12}, R_{MM} in (24) and S_{11}, S_{12}, S_{MM} in (25) are easily obtained from the magnetic circuits in Fig. 3(b).

When we compare the magnetic circuits in Fig. 3(b) with (17)-(25), then it is found that the loop magnetic flux ϕ_{M+1} [shown by dotted line in Fig. 3(b)] must be taken into account in the calculation of magnetic fluxes to satisfy the condition of minimum number of network equations [6]. Since the loop magnetic flux ϕ_{M+1} in Fig. 3(b) is physically flowing toward the tangential direction on the center of the radial direction, we can find the following relationship:

$$\Phi[t] = C^T \Phi^c[t] \ , \tag{26}$$

where superscript c refers to the three-dimensional quantities, and C^T is the magnetic flux connection matrix which is a rectangular matrix with M rows and M+1 columns, that is

$$C^T = \begin{vmatrix} 1 & 0 & 0 & . & -1 \\ 0 & 1 & 0 & . & -1 \\ . & . & . & . & . \\ 0 & 0 & 0 & . & -1 \end{vmatrix} . \tag{27}$$

By means of the magnetic power invariant transformation method [5], the system of three-dimensional magnetic circuit equations is derived by

$$F^c[t] = CF[t] = Z^c[t]\Phi^c[t] \ , \tag{28}$$

where

$$Z^c[t] = CZ[t]C^T = R^c[t] + (S^c[t] + G^c)\left(\frac{d}{dt}\right) . \tag{29}$$

NUMERICAL METHOD OF SOLUTION

In order to discretize the time differential terms in (28), a finite difference method is applied to (28), that is

$$F^c[\alpha] = R^c[\alpha]\{\alpha\Phi^c[t+\Delta t] + (1-\alpha)\Phi^c[t]\} + \{G^c + S^c[\alpha]\}(1/\Delta t)\{\Phi^c[t+\Delta t] - \Phi^c[t]\} \ , \tag{30}$$

where

$$F^c[\alpha] = \alpha F^c[t+\Delta t] + (1-\alpha)F^c[t] \ ,$$
$$R^c[\alpha] = \alpha R^c[t+\Delta t] + (1-\alpha)F^c[t] \ , \tag{31}$$
$$S^c[\alpha] = \alpha S^c[t+\Delta t] + (1-\alpha)S^c[t] \ ,$$

The parameter α in (30),(31) can be chosen arbitrarily e.g. $\alpha=0$, $\alpha=1$ yield forward, backward differences; and Δt denotes the stepwidth in time.

To evaluate the magnetic flux vector $\Phi^c[t+\Delta t]$ from (30), an iteration method using a relaxation parameter ω is applied to (30). As shown in Fig. 4, the relaxation parameter ω is sequentially determined in every complete iteration.

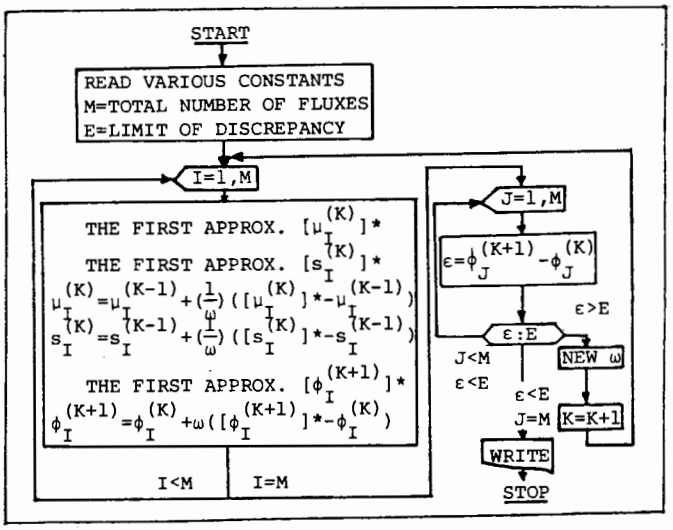

Fig. 4. Flow chart of the iteration method.

The relaxation parameter ω is determined by the following assumptions:

$$1 \leq \omega < 2 \ , \tag{32}$$

$$\varepsilon = f(\omega) \ , \tag{33}$$

where $f(\omega)$ means that the mean percentage error ε for entire solutions is a function of ω. When the relaxation parameter $\omega+\Delta\omega$ which satisfies the condition of (32) is selected to the most suitable value, then the error $\varepsilon=f(\omega+\Delta\omega)$ reduces to

$$f(\omega+\Delta\omega) \simeq f(\omega) + \Delta\omega\frac{\partial f}{\partial \omega} = 0 \ . \tag{34}$$

The term $\partial f/\partial\omega$ in (34) is replaced by the divided difference, therefore, it is possible to determine the most suitable relaxation parameter in every complete iteration [4].

NUMERICAL SOLUTIONS

The theory of magnetic circuits is applicable to the magnetic field calculations of all electromagnetic devices. In order to demonstrate the dynamic hysteresis loops as well as eddy currents in an iron core, this paper examines the magnetic fields of a simple saturable reactor as an example.

Figure 5 shows the magnetization curves used in the calculations. In carrying out the magnetic field computations of the saturable reactor, the magnetization curves of iron are introduced by the linear interpolations.

First, the parameter α and Δt in (30),(31) are respectively determined as $\alpha=0.5$ and $\Delta t \leq 0.25$(msec) by the numerical tests when the convergence and accuracy

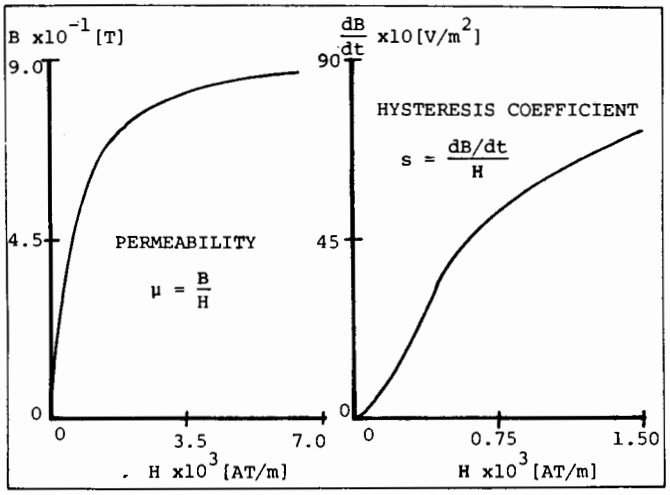

Fig. 5. Magnetization curves used in the calculations.

Table 1. Various constants used in the calculations.

Number of Subdivisions in Radial Direction		6
Number of Subdivisions in Tangential Direction		8
Limit of Discrepancy		0.1 Percent
Inner Radius of Iron Core		0.04 [m]
Outer Radius of Iron Core		0.05 [m]
Thickness of Iron Core		0.01 [m]
Thickness of Exciting and Search Coils		0.002 [m]
Thickness of the Region Containg Air		0.05 [m]
Number of Turns of Exciting Coil,	3-D Model	400
	1-D Model	900
Number of Turns of Search Coil,	3-D Model	200
	1-D Model	900
Electric Resistance of Exciting Coil,		
3-D Model	Laminated Core	5.57 [Ω]
	Solid Core	4.91 [Ω]
1-D Model		6.30 [Ω]
Conductivity of Iron Core		1/20.6 [1/μΩcm]
All the initial magnetic fluxes and currents are set to zero		

of the solutions are taken into account.

Second, in order to check the accuracy of the magnetization curves of Fig. 5, comparisons of the experimental and computational results are carried out for the one-dimensional model. When we assume that the region containing air is divided into M_R parts in the radial direction while the region containing iron is not divided in the radial direction, and that the loop magnetic fluxes which are flowing through the path containing air can be neglected, then the magnetic circuits shown in Fig. 3(b) is reduced to the one-dimensional model. The magnetization curves of Fig. 5 were measured from this one-dimensional model. The iron core of this one-dimensional model was constructed from laminated steels to suppress the eddy currents. Also, the exciting and search coils of this model were alternatively arranged to reduce the leakage magnetic fluxes from an iron core. As shown in Fig. 6, fairly good agreements between the experimental and computational results are obtained under the steady state as well as transient state conditions.

Third, comparisons of the experimental and computational results were made for the three-dimensional model with laminated core. These results are shown in Fig. 7. Since the experimental model which produced the results in Fig. 7 was constructed from laminated steels, the experimental model did not rigorously correspond to the computational model. For example, the cross-sectional area of the experimentally used iron core is about 10 percent greater than those of the iron core used in the calculations. This means that

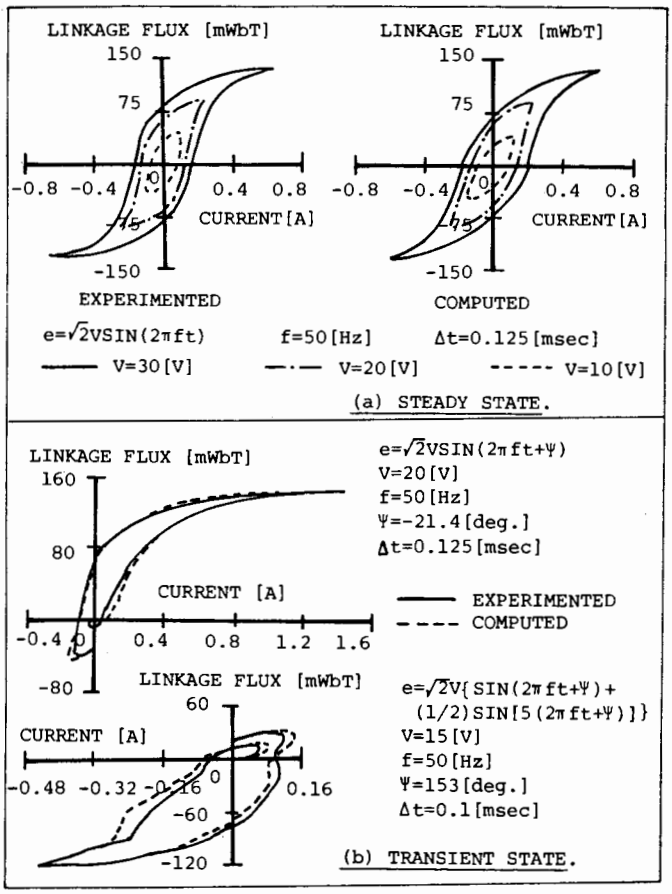

Fig. 6. One-dimensional model.

the magnetic fluxes obtained from the experimental model may take the greater values when compared with those of computed values. Moreover, the laminated core of the experimental model essentially makes the magnetization characteristics of iron anisotropic in direction, but it is assumed that the magnetization characteristics of iron used in the calculations are the isotropic properties. Therefore, the discrepacies between the experimental and computational results in Fig. 7 are not necessarily small values compared with those of Fig. 6.

Finally, comparisons of the experimental and computational results were made for the three-dimensional model with solid iron core. Since the experimental model in this case rigorously corresponds to the computational model, as shown in Fig. 8, fairly good agreements between the experimental and computational results are obtained.

When we consider the results in Figs. (7),(8), then it is obvious that the dynamic hysteresis loops are considerably dominated by the eddy currents.

CONCLUSION

As shown above, in this paper, a new magnetic field equation exhibiting the dynamic hysteresis loops has been proposed. As an example, the three-dimensional dynamic hysteresis loops in a simple saturable reactor has been clarified. The operation count required for the results in Fig. 8(b) was about 5 minutes on the computer ACOS-6/SYSTEM 700 at the Computer Center of Hosei University.

ACKNOWLEDGEMENT

The author is grateful to Professor I. Fujita and Professor T. Yamamura for their helpful advice. The assistance of Mr.H. Saotome is gratefully acknowledged.

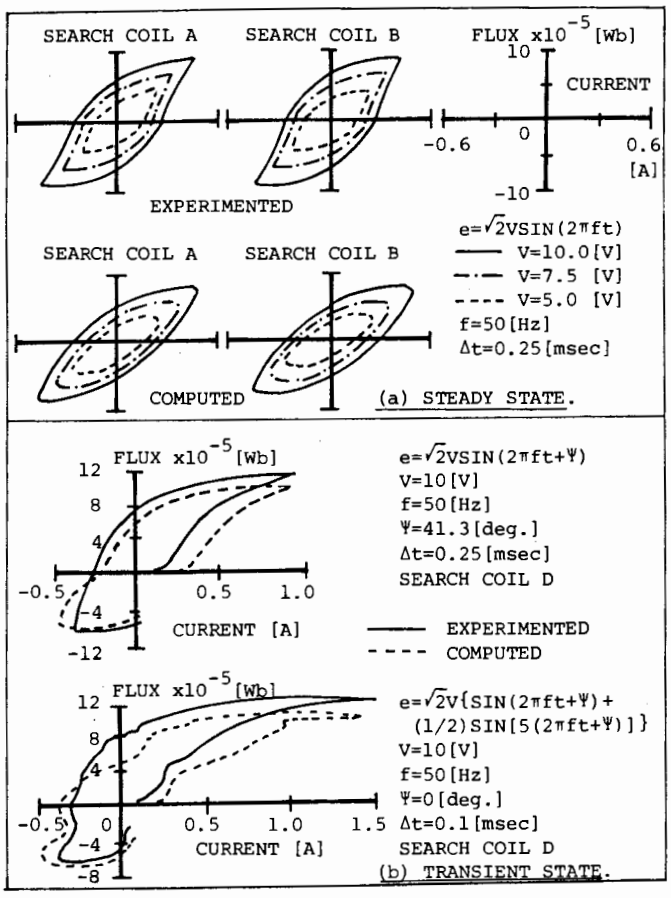

Fig. 7. Three-dimensional model with laminated core.

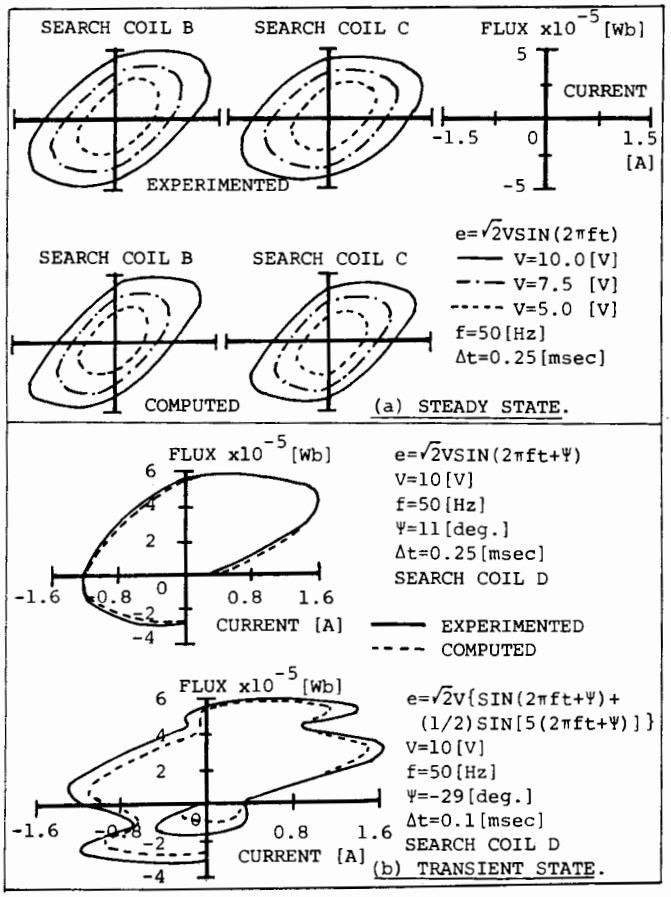

Fig. 8. Three-dimensional model with solid core.

APPENDIX

Basic equations governing the electromagnetic fields are generally written by

$$\nabla\times H = J\ ,\qquad \nabla\times E = -\left(\frac{\partial B}{\partial t}\right),\qquad J = \sigma E\ ,\qquad \nabla\times A = B\ , \tag{A.1}$$

where J,E,A,σ are respectively the current density, electric field intensity, vector potential and conductivity of the material. By combining (A.1) with (5), it is possible to obtain

$$\nabla\times\left\{\left(\frac{1}{\mu}\right)\nabla\times A\right\}+\nabla\times\left\{\left(\frac{1}{s}\right)\left(\frac{\partial}{\partial t}\nabla\times A\right)\right\} = \sigma\left(E_e-\frac{\partial A}{\partial t}\right)\ , \tag{A.2}$$

where E_e is the externally impressed electric field intensity. For simplicity, let consider the two-dimensional rectangular coordinate system, then (A.2) reduces to

$$\frac{\partial}{\partial x}\left\{\frac{1}{\mu}\frac{\partial A}{\partial x}\right\}+\frac{\partial}{\partial y}\left\{\frac{1}{\mu}\frac{\partial A}{\partial y}\right\}+\frac{\partial}{\partial x}\left\{\frac{1}{s}\left(\frac{\partial}{\partial t}\right)\frac{\partial A}{\partial x}\right\}+\frac{\partial}{\partial y}\left\{\frac{1}{s}\left(\frac{\partial}{\partial t}\right)\frac{\partial A}{\partial y}\right\}$$
$$= -\sigma\left\{E_e-\frac{\partial A}{\partial t}\right\}\ , \tag{A.3}$$

where A,E_e are respectively z-components of the vector potential and of the externally impressed electric field intensity. With h,g denoting the mesh spacings in x and y directions, (A.3) is replaced by the following magnetic circuit equation

$$\sum_{i=2}^{3}\left\{\left(\frac{g}{hq}\right)\left[\frac{1}{\mu_{1i}}+\frac{1}{s_{1i}}\left(\frac{\partial}{\partial t}\right)\right](\phi_1-\phi_i)\right\}+\sum_{i=4}^{5}\left\{\left(\frac{h}{gq}\right)\left[\frac{1}{\mu_{1i}}+\right.\right.$$
$$\left.\left.\frac{1}{s_{1i}}\left(\frac{\partial}{\partial t}\right)\right](\phi_1-\phi_i)\right\} = \sigma\left(\frac{gh}{q}\right)\left[e_1-\frac{\partial\phi}{\partial t}1\right], \tag{A.4}$$

where q denotes the unit length in the direction of z-axis; $\phi_i=qA_i$, i=1,2,3,4,5; and $e_1=qE_e$. By considering (A.4), it is revealed that (A.4) is one of the finite difference equations.

REFERENCES

[1] S.H. Charap, "Magnetic Hysteresis Model," IEEE Trans. Magnetics, Vol. MAG-10, 1974, pp. 1091-1096.

[2] L.O. Chua and K.A. Stomsmoe,"Lumped-Circuit Model for Nonlinear Inductors Exhibiting Hysteresis Loops," IEEE Trans. Circuit Theory, Vol. CT-17, No. 4, 1970, pp. 564-574.

[3] L.O. Chua and S.C. Bass, "A Generalized Hysteresis Model," IEEE Trans. Circuit Theory, Vol. CT-19, No. 1, 1972, pp. 36-48.

[4] Y. Saito, "Three-Dimensional Analysis of Nonlinear-magnetostatic Fields in a Saturable Reactor,"Comp. Meths. Appl. Mech. Eng., Vol. 16, No. 1, Oct. 1978, pp. 101-115.

[5] Y. Saito, "Three-Dimensional Analysis of Nonlinear-magnetodynamic Fields in a Saturable Reactor," Comp. Meths. Appl. Mech. Eng., Vol. 22, No. 3, June 1980, pp. 289-308.

[6] H.K. Messerle, Dynamic Circuit Theory. Oxford: Pergamon, 1965, pp. 117-167.